View Online

Controlled fabrication of SnO_2 arrays of well-aligned nanotubes and nanowires

Liang Shi,*[a] Yeming Xu[b] and Quan Li[b]

Received 26th April 2010, Accepted 17th May 2010
DOI: 10.1039/c0nr00279h

Highly oriented SnO_2 nanotubes and nanowires arrays have been selectively fabricated *via* a convenient one-step wet-chemical approach using anodic aluminium oxide (AAO) as a hard template. Wall thickness of the SnO_2 nanotubes was tunable. The as-prepared nanostructures were composed of fine particles with sizes as small as 5 nm. Formation mechanism of SnO_2 nanostructure arrays with different shape is also discussed based on the experimental results. The structure, morphology, composition properties of the as-prepared samples were characterized using X-ray powder diffraction, transmission electron microscopy, energy dispersive X-ray spectrometry, scanning electron microscopy and Raman spectrum.

Published on 05 August 2010 on http://pubs.rsc.org | doi:10.1039/C0NR00279H
Downloaded on 02 March 2011

1. Introduction

As a stable and n-type large bandgap semiconductor, tin oxide (SnO_2) has excellent optical and electrical properties such as peculiar optical transparency, low resistivity, and high theoretical specific capacity. It has been widely used as gas sensors, heat mirrors, glass coatings, photocatalysts, transparent electrodes for solar cells and storage applications. One dimensional (1D) nanomaterials of SnO_2 have been found to exhibit peculiar chemical and optoelectronic properties due to their direct channels for efficient electron transport.[1–5] Over the past several years, various 1D nanostructured SnO_2 including nanorods, nanowires, nanoribbons and nanobelts have been prepared successfully.[6–11] On the other hand, the fabrication of arrays of well-aligned 1D semiconductor nanostructure (nanowire, nanotube or nanorod) with intensified anisotropy are highly desirable because it is a key step toward building functional nanodevices such as nanoscale electronics and molecular sensing, field-effect transistors, and electron emitters.[12–15] Arrays of some 1D semiconductors including ZnO and CuO have been fabricated,[16–18] and they were found to exhibit excellent photolumincence, field–emission and sensing properties.

Up to now, there have been a few reports about the preparation of SnO_2 arrays of well-aligned one dimensional (1D) nanostructures with approaches such as chemical vapor deposition and sol–gel methods.[19–21] Some of these reported approaches require either high energy consumption or a relative complicated procedure. The template method is one of the most efficient methods for the fabrication of highly ordered well-distributed one-dimensional nanomaterials, especially for nanotubes and nanowires.[22,23] Here we report a facile one-step solution AAO template-assisted method for growing uniform well aligned SnO_2 1D nanostructure arrays at a low temperature. In particular, it is known that controlled fabrication of nanostructures with desired shapes plays an important role in both nanomaterials science and technology. Our present solution approach allows us to shape selectively synthesize nanotubes and nanowires array and tune the wall thickness of nanotubes by simply modifying the reaction time.

2. Experimental section

All reagents are analytical grade and used without further purification. AAO templates (Whatman Co., U.K.) with pore sizes of 100 nm in diameter were used in the experiments. In a typical procedure, for the fabrication of SnO_2 nanotube array within the AAO template, a 20 mL precursor solution was made by introducing 0.09 g K_2SnO_3 $3H_2O$ (Aldrich, 99.9%), 0.5 g urea, 8 mL ethanol and 12 mL distilled water to a 25 mL flask in air with magnetic stirring until a transparent solution appeared. Then, an AAO template was added into the flask and immersed in the liquid. The above liquid mixture in the flask was treated by sonication for 5 min to remove air in the pore of AAO template and fill the pore with liquid. The flask was attached to a Schlenk line and purged of air by pulling vacuum for 10 min, followed by nitrogen bubbling for 10 min with mild magnetic stirring. The evacuation and N_2 bubbling process was cycled for 3 times at room temperature. The sonication and multi-evacuation and bubbling process was important to enhance the filling efficiency of the AAO template pores with mixture of reaction solution. As a result, a uniform and high density of nanotubes array can be obtained. The above solution in the flask was then transferred into a 20 mL stainless steel teflon-lined autoclave. The autoclave was sealed and the temperature was maintained at 200 °C for 16 h before being cooled down to room temperature. The AAO template containing the product was take out, thoroughly washed with ethanol and distilled water, air-dried for characterization.

The overall crystallinity of the product is examined by X-ray diffraction (XRD, Rigakau RU-300 with Cu-Kα radiation). The general morphology of the products was characterized using scanning electron microscopy (FESEM QF400). Detailed microstructure analysis was carried using transmission electron microscopy (TEM Tecnai 20ST). The chemical composition

[a]*Department of Chemistry, University of Science and Technology of China, Hefei 230026, P. R. China. E-mail: sliang@ustc.edu.cn.; Fax: +86-551-3607402; Tel: +86-551-3607234*
[b]*Department of Physics, The Chinese University of Hong Kong, Shatin, New Territory, Hong Kong, P. R. China*

 This journal is © The Royal Society of Chemistry 2010

View Online

Published on 05 August 2010 on http://pubs.rsc.org | doi:10.1039/C0NR00279H
Downloaded on 02 March 2011

analysis was obtained by energy dispersive X-ray spectrometry (EDX) using an EDX spectrometer attached to the same microscope. Room-temperature Raman spectra were measured using a micro-laser Raman spectrometer (Renishaw) in a back-scattering configuration, employing the 514.5 nm line of Ar laser as the excitation source. For the SEM measurements, several drops of 1 M NaOH aqueous solution were added onto the sample to dissolve some part of the AAO template. The residual solution on the surface of the template was rinsed with distilled water. For the TEM and HRTEM measurements, the template was completely dissolved in 2M NaOH aqueous solution. The product was centrifuged, thoroughly washed with distilled water to remove residual NaOH and then rinsed with absolute ethanol.

3. Results and discussion

The crystal structure of the product was firstly characterized by X-ray diffraction (XRD). A typical XRD pattern of the as-prepared SnO_2 product embedded in AAO pores is shown in Fig. 1. All diffraction peaks can be indexed to the rutile structured SnO_2 with tetragonal lattice constant $a = 4.738$ Å and $c = 3.186$ Å, which match well to the reported value for SnO_2 crystal (JCPDS card, No. 41-1445). No signals of impurities or side products were found in the product. Due to the diffraction of amorphous AAO hard template, an increasing background at small diffraction angles can be found in the XRD pattern. The obviously broadening of XRD peaks suggests that the as-prepared SnO_2 crystals are of very small sizes. Based on the Scherrer equation, $D = (0.89\lambda)/\beta(\cos\theta)$, here λ is the wavelength for the $K\alpha_1$ (1.54056 Å), β is the peak width at half-maximum in radians and θ is the Bragg's angle, the average particle size was calculated to be 5.3 nm. The particle size result is consistent with the further structural analysis in later sections.

Fig. 2 shows typical SEM images of the SnO_2 product with AAO template partially removed. Large-area continuous, smooth, high ordered dense nanotubes array can be seen in Fig. 2a. These nanotubes are all straight and parallel to each other and oriented vertically to the surface of the AAO template. A magnified image in Fig. 2b shows clearly that the hollow tube structure of the sample. The size distribution of the as prepared nanotubes are all uniform over the entire area and the average diameter of the nanowires is about 100 nm, which is consistent

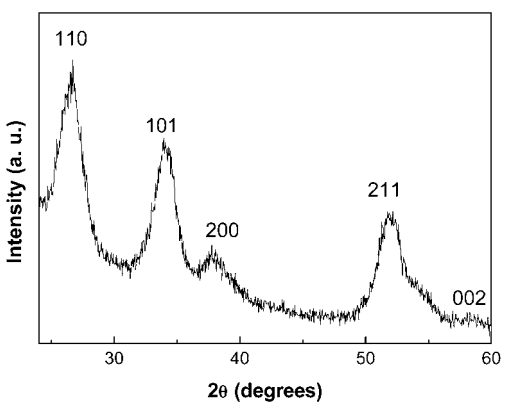

Fig. 1 A representative XRD pattern of the as-prepared SnO_2 nanostructures.

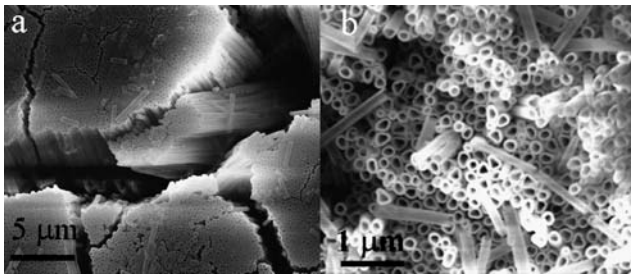

Fig. 2 SEM images of the as-prepared SnO_2 nanotubes array: (a) overview; (b) magnified image showing clear hollow tube structure.

with the pore size dimension of the AAO template. Some isolated nanotubes originated from the breakage of long nanotubes lie on the top of the array. These isolated nanotubes are straightforward though they are several micrometres long, indicating the structurally robust and well preserved.

Detailed microstructure information and chemical composition of individual nanowire are obtained through TEM studies accompanied by selected area electron diffraction (SAED) and energy dispersive X-ray spectrometry (EDX). A TEM image in Fig. 3a indicates that the as-prepared nanotubes are straight with smooth surface. The average thickness of the SnO_2 nanotubes is estimated to be about 10 nm. The diffraction rings of the SAED pattern for the product, as displayed in the inset of Fig. 2a, reveals that the nanotubes are polycrystalline. The brightest diffraction ring can be indexed to (110) planes. The strong (110) ring suggests the crystals have a preferred growth orientation. A HRTEM image (Fig. 3b) shows that the as-prepared nanotubes consist of small nanocrystalline grains with an average size of about 5 nm, displaying their polycrystalline structure. As shown in Fig. 3b, the lattice fringe spacings of each crystalline grain are measured to be 0.335 nm, matching the d value for (110) planes of rutile SnO_2. The HRTEM image discloses the wall thickness of the nanotube is about 10 nm, which is consistent with the above observation in TEM image in Fig. 3a. The EDX spectrum (Fig. 3c) from the product shows intense peaks of Sn and O, displaying the composition as Sn and O only. The Cu and carbon signals come from the supporting TEM grid. EDX quantitative analysis gives an average Sn/O composition of 1 : 2 within the accuracy of the technique, in accordance with the stoichiometry of SnO_2.

Raman scattering spectroscopy was employed to study the vibrational properties of the as-prepared SnO_2 nanotube array. Fig. 4 shows a typical room-temperature Raman spectrum for the SnO_2 product in the range of 400–900 cm^{-1}. Vibration peaks can be clearly observed at 472, 632, 696, 722 and 774 cm^{-1}. The 472 cm^{-1} peak can be assigned to E_g mode, which is related to the vibration of oxygen in the oxygen plan.[24] The 632 and 774 cm^{-1} peak can be assigned to A_{1g} and B_{2g} vibration modes respectively, which are induced by the expansion and contraction vibration mode of Sn–O bonds and usually appear in bulk single crystals or polycrystalline SnO_2 materials.[25] These Raman features give evidence that the as-synthesized SnO_2 nanotubes possess the features of the tetragonal rutile structure. Besides these normal classical vibration modes, two additional Raman scattering peaks at 696 and 722 cm^{-1} appear also in the pattern. These two peaks are believed to originate from space symmetry

View Online

Published on 05 August 2010 on http://pubs.rsc.org | doi:10.1039/C0NR00279H
Downloaded on 02 March 2011

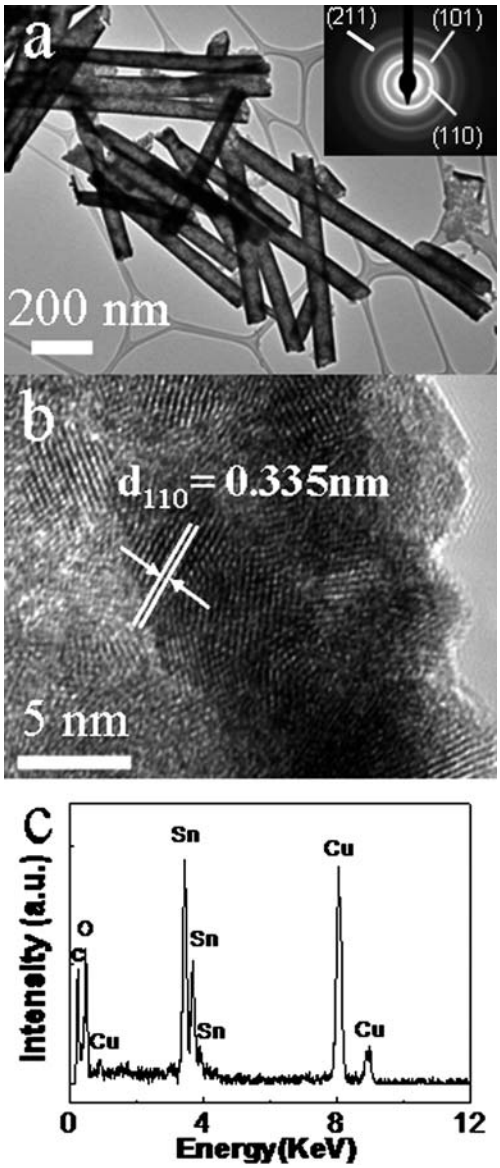

Fig. 3 TEM (a), SAED (inset of a), HRTEM (b) images and EDX spectrum (c) of the as-prepared SnO_2 nanotube array.

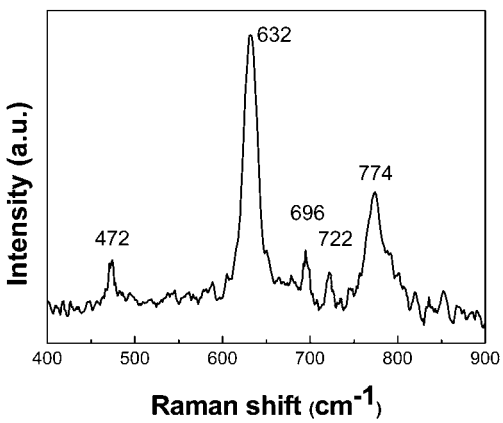

Fig. 4 A typical room-temperature Raman spectrum of the as-prepared SnO_2 nanotubes array.

of the nanoscale SnO_2 grain assemblage relating to existence of vacant lattice sites and local lattice disorder. This discloses the very small size of SnO_2 nanocrystals in the nanotubes.[26]

It is found that the reaction time has a significant influence on the wall thickness of the SnO_2 nanotubes. If the reaction time was extended to 24 h with other reaction conditions unchanged, a SnO_2 nanotubes array could still be obtained, as shown in the SEM image of Fig. 5a. However, the wall thickness of the nanotubes is found to increase remarkably to be about 30 nm. A TEM image in Fig. 5b shows clear hollow nanotube structure of the sample and the wall thickness of the nanotube is about 30 nm. This is consistent with the SEM observation result. The SAED pattern in the inset of Fig. 5b indicates that the as-prepared nanotubes are polycrystalline. The EDX spectrum in Fig. 5c shows its chemical composition of only Sn and O. A HRTEM image (Fig. 5d) shows crystalline domains and confirm its polycrystalline nature. The clear lattice spacing of 0.335 nm of one domain can be indexed as (110) planes of rutile SnO_2.

If the reaction time was extended further to 40 h, the final product became nanowires array, instead of nanotubes array. Fig. 6a illustrates a SEM image of the as-prepared sample with the template partially removed. A large area array of uniformly distributed well aligned nanowires can be found in the sample. Fig. 4b gives a TEM image, indicating that the as-prepared clean solid nanowires have a diameter of about 100 nm. SAED pattern (inset of the Fig. 6b) shows diffraction rings, disclosing the polycrystalline character of the as-prepared SnO_2 nanowires. The EDX (Fig. 6c) and HRTEM (Fig. 6d) results prove together these nanowires are pure SnO_2 and polycrystalline, similar to that of nanotubes array.

A typical room-temperature Raman spectrum for the SnO_2 nanowires array in the range of 400–900 cm^{-1} is shown in Fig. 7. Vibration peaks centered at around 472, 632, 696, 722 and

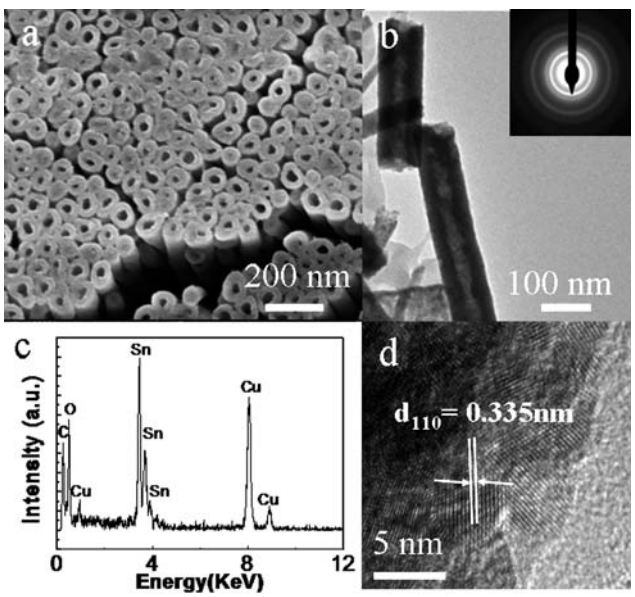

Fig. 5 SEM (a), TEM (b), SAED (inset of b), HRTEM (d) images and EDX spectrum(c) of the SnO_2 nanotubes array with increased wall thickness of the nanotubes.

This journal is © The Royal Society of Chemistry 2010

View Online

Published on 05 August 2010 on http://pubs.rsc.org | doi:10.1039/C0NR00279H
Downloaded on 02 March 2011

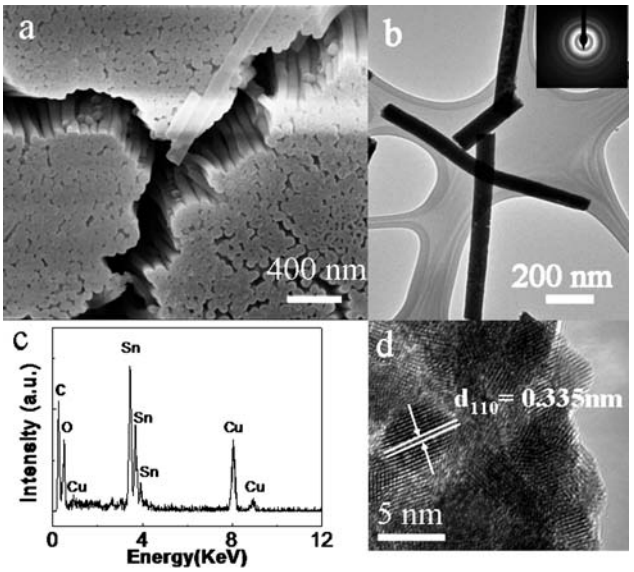

Fig. 6 SEM (a), TEM (b), SAED (inset of b), HRTEM (d) images and EDX spectrum (c) of the as-prepared SnO_2 nanowires array.

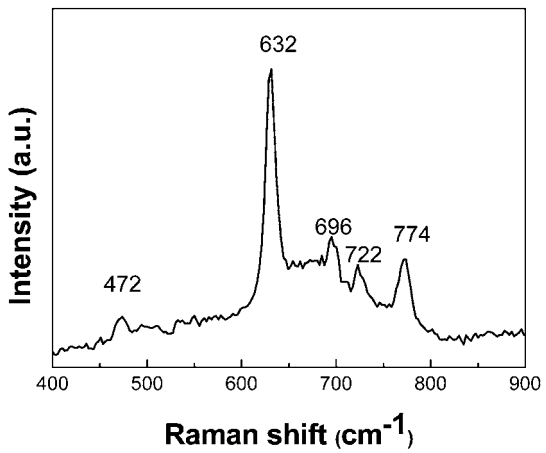

Fig. 7 A typical room-temperature Raman spectrum of the as-prepared SnO_2 nanowires array.

774 cm^{-1} can all be observed, similar to the Raman spectra of SnO_2 nanotubes array. This confirms the product of SnO_2 and its very small size of nanocrystals in the nanowires.

Based on above experimental results, a possible formation mechanism of SnO_2 nanotubes and nanowires arrays could be proposed as follows. During the reaction process, AAO templates were immersed in the reaction solution. The sonication and multi-cycles of evacuation and bubbling process ensure removal of gas from the AAO template pores and filling them with reaction solution by negative pressure and capillary action. In the precursor solution, the K_2SnO_3 tends to hydrolyze as follows,

$$K_2SnO_3 + 2H_2O \rightarrow H_2SnO_3\downarrow + 2KOH \quad (1)$$

With the increase of temperature during the reaction process, the hydrolysis reaction was promoted. When the temperature was higher than 60 °C, urea began to hydrolyze as eqn (2),

$$(NH_2)_2CO + 3H_2O \rightarrow 2NH_4^+ + 2OH^- + CO_2 \quad (2)$$

The PH value of the solution rose and led to a strong basic environment. Excess OH^- ions reacted with H_2SnO_3 and formed $[Sn(OH)_6]^{2-}$. The pore walls of AAO are known to be positively charged due to the presence of a layer of acidic anions held either covalently or present as hydrated anions (complex anions $Al(H_2O)_4(OH)^+_2$ and $Al(H_2O)_4^+$).[27] Therefore, $[Sn(OH)_6]^{2-}$ ions attached to the pore wall preferably and then reacted with CO_2 originating from the urea hydrolysis and induced deposition of SnO_2 on the AAO pore walls based on the following reaction 3,

$$[Sn(OH)_6]^{2-} + CO_2 \rightarrow SnO_2 + CO_3^{2-} + 3H_2O \quad (3)$$

Along with the reaction processed, heterogeneous nucleation occurred at the surfaces of the pore walls and accompanying crystal growth started here under confinement of the pore walls geometry. With the assembly of the as-formed particles, the final product would be tubes with outer diameter determined by the pore diameter in the AAO template. Since the crystal growth started from the inner surface of pore walls and extend to the center, the thickness would become thicker if the reaction is prolonged. This is in accordance with our experimental result when the reaction time was extended to 24 h. As an extreme case, the AAO pore could be filled completely and form solid nanowires with the continuous lateral thickening due to enough long time reaction.

In summary, a novel convenient one-step hydrothermal approach has been developed for controlled fabrication of large scale SnO_2 nanotubes and nanowires arrays. During the reaction process, AAO is used as a shape directing template. By simple changing the reaction duration, desired shape of nanotubes or nanowires product can be obtained. In addition, the wall thickness of as-prepared nanotubes can also be modified. A growth mechanism of SnO_2 nanotubes and nanowires arrays is also proposed. The present synthesis strategy may be extended to controllably prepare other high ordered array of one dimensional oxide nanostructures.

Acknowledgements

The financial support of this work by the National Natural Science Foundation of China (Grant No. 20771096) and the 973 Project of China (no. 2005CB623601) is gratefully acknowledged.

References

1 M. S. Park, G. X. Wang, Y. M. Kang, D. Wexler, S. X. Dou and H. K. Liu, *Angew. Chem., Int. Ed.*, 2007, **46**, 750–753.
2 G. C. Xi and J. H. Ye, *Inorg. Chem.*, 2010, **49**, 3553–3553.
3 D. W. Kim, I. S. Hwang, S. J. Kwon, H. Y. Kang, K. S. Park, Y. J. Choi, K. J. Choi and J. G. Park, *Nano Lett.*, 2007, **7**, 3041–3045.
4 Z. Ying, Q. Wan, H. Cao, Z. T. Song and S. L. Feng, *Appl. Phys. Lett.*, 2005, **87**, 113108.
5 Y. Wang and J. Y. Lee, *J. Phys. Chem. B*, 2004, **108**, 17832–17837.
6 J. Liu, F. Gu, Y. J. Hu and C. Z. Li, *J. Phys. Chem. C*, 2010, **114**, 5867–5870.
7 Y. L. Wang, X. C. Jiang and Y. N. Xia, *J. Am. Chem. Soc.*, 2003, **125**, 16176–16177.
8 H. G. Yang and H. C. Zeng, *Angew. Chem., Int. Ed.*, 2004, **43**, 5930–5933.
9 Z. W. Pan, Z. R. Dai and Z. L. Wang, *Science*, 2001, **291**, 1947–1949.

View Online

10 B. Cheng, J. M. Russell, W. S. Shi, L. Zhang and E. T. Samulski, *J. Am. Chem. Soc.*, 2004, **126**, 5972–5973.
11 L. Zhao, M. Yosef, M. Steinhart, P. Goring, H. Hofmeister, U. Gosele and S. Schlecht, *Angew. Chem., Int. Ed.*, 2006, **45**, 311–315.
12 M. H. Huang, S. Mao, H. Feick, H. Yan, Y. Wu, H. Kind, E. Weber, R. Russo and P. Yang, *Science*, 2001, **292**, 1897–1899.
13 M. Law, L. E. Greene, J. C. Johnson, R. Saykally and P. Yang, *Nat. Mater.*, 2005, **4**, 455–459.
14 Z. L. Wang and J. Song, *Science*, 2006, **312**, 242–246.
15 L. Vayssieres, K. Keis, S.-E. Lindquist and A. Hagfeldt, *J. Phys. Chem. B*, 2001, **105**, 3350–3352.
16 L. Vayssieres, *Adv. Mater.*, 2003, **15**, 464–466.
17 X. G. Wen, W. X. Zhang and S. H. Yang, *Langmuir*, 2003, **19**, 5898–5903.
18 L. Vayssieres and M. Graetzel, *Angew. Chem., Int. Ed.*, 2004, **43**, 3666–3670.
19 N. H. Zhao, G. J. Wang, Y. Huang, B. Wang, B. D. Yao and Y. P. Wu, *Chem. Mater.*, 2008, **20**, 2612–2614.
20 Y. Liu and M. L. Liu, *Adv. Funct. Mater.*, 2005, **15**, 57–62.
21 Y. Liu, J. Dong and M. L. Liu, *Adv. Mater.*, 2004, **16**, 353–356.
22 T. A. Crowley, K. J. Ziegler, D. M. Lyons, D. Erts, H. Olin, M. A. Morris and J. D. Holmes, *Chem. Mater.*, 2003, **15**, 3518–3522.
23 O. Rabin, P. R. Herz, Y. M. Lin, A. I. Akinwande, S. B. Cronin and M. S. Dresselhaus, *Adv. Funct. Mater.*, 2003, **13**, 631–638.
24 F. Gervais and W. Kress, *Phys. Rev. B: Condens. Matter*, 1985, **31**, 4809–4814.
25 R. S. Katiyar, P. Dawson, M. M. Hargreave and G. R. Wilkinson, *J. Phys. C: Solid State Phys.*, 1971, **4**, 2421–2431.
26 K. N. Yu, Y. H. Xiong, Y. L. Liu and C. S. Xiong, *Phys. Rev. B: Condens. Matter*, 1997, **55**, 2666–2671.
27 J. W. Diggle, T. C. Downie and C. W. Goulding, *Chem. Rev.*, 1969, **69**, 365–405.

Published on 05 August 2010 on http://pubs.rsc.org | doi:10.1039/C0NR00279H
Downloaded on 02 March 2011

 This journal is © The Royal Society of Chemistry 2010